Desalination and Water Treatment
www.deswater.com
doi: 10.1080/19443994.2014.963156

56 (2015) 3087–3095
December

Taylor & Francis
Taylor & Francis Group

UV/persulfate and UV/hydrogen peroxide processes for the treatment of salicylic acid: effect of operating parameters, kinetic, and energy consumption

J. Saien[a,*], M. Osali[a], A.R. Soleymani[b]

[a]*Department of Applied Chemistry, Bu-Ali Sina University, Hamedan 65174, Iran, Tel./Fax: +98 81 38257407; email: saien@basu.ac.ir (J. Saien), Tel. +98 91 25423586; email: m.osali0241@gmail.com (M. Osali)*
[b]*Department of Applied Chemistry, Malayer University, Malayer 65719, Iran, Tel. +98 91 66991400; email: solyman_1359@yahoo.com (A.R. Soleymani)*

Received 14 February 2014; Accepted 2 September 2014

ABSTRACT

Two advanced oxidation processes (AOPs), based on UV light irradiation with potassium persulfate (UV/KPS) and with hydrogen peroxide (UV/H_2O_2), were employed for the treatment of salicylic acid (SA) in aqueous media. The influence of operating parameters, initial pH and concentration of the oxidant reagents, was investigated. Under the optimum conditions of pH 6 and [KPS] = 1,000 mg/L for UV/KPS and pH 4 and [H_2O_2] = 140 mg/L for UV/H_2O_2, about 94 and 98% SA degradations were achieved after 60 min treatments. Total organic carbon removal was also obtained as 80% and 87%, respectively, after 150 min. Rate of SA degradation in these processes obeys pseudo-first-order kinetic. For UV/KPS process, the role of active radicals was studied using ethanol and tert-butyl alcohol radical scavengers, indicating the contribution of hydroxyl and sulfate radicals in the degradation of about 56% and 44%, respectively. The electrical energy consumption, for nearly complete degradation of SA, was evaluated and the preference was shown in comparison with previous works.

Keywords: Salicylic acid; UV/KPS; UV/H_2O_2; Kinetic; Energy consumption

1. Introduction

There is currently much attention paid to improving the pharmaceutical pollutants treatment in the aqueous media. These chemicals enter water sources via industry wastewaters or solid waste land fillings [1]. Some pharmaceuticals persist against biological degradation and have a physiological effect on human and animals in trace amounts [2]. Although dosage of these chemicals in aquatic systems is low, but their continuous input, in the long term, may lead to accumulations in aqueous media, causing environmental problems [3].

Salicylic acid (SA), also known as 2-hydroxybenzoic acid, is widely used as an intermediate in the manufacture of pharmaceuticals and cosmetics and is widely present in pharmaceutical industrial effluents [4]. It is a key ingredient in many skin care products for the treatment of acne, psoriasis, calluses, corns, keratosis, and warts; and therefore, it is introduced into the environment by a variety of industrial sources. The toxic effects of SA and salicylates are complex. For this substrate, the announced amount of margin of

---

*Corresponding author.

safety, which is based on the most critical limit, is 0.35 μg/L [5].

AOPs are generally proposed as the most promising and effective methods for the treatment of water containing hazardous materials, refractory, and non-biodegradable organic pollutants. Over the past few decades, different AOPs have been employed, including Fenton and Fenton-like processes and photo-irradiation in the presence of potassium persulfate (UV/KPS) or hydrogen peroxide (UV/H_2O_2) processes as well as different methods in photocatalytic treatments [6–9]. In these processes, generated reactive radicals, $SO_4^{\cdot-}$ and $HO^{\cdot}$ radicals with oxidation potentials of 2.6 and 2.8 V, play main roles in removing organic pollutants. In UV/KPS treatment, sulfate ions will be generated as the end product [10], which causes a decrease in pH and of course, an increase in the effluent salt content or total dissolved solids. However, the sulfate ion has environmentally low risk. The United States Environmental Protection Agency has listed it under the secondary drinking water standards with a maximum allowed concentration of 250 mg/L (1.43 mM) [11]. Meanwhile, in UV/H_2O_2 process, only $HO^{\cdot}$ radical is dominant. Briefly, generation of the radicals has been described via the following reactions [12,13]:

$$S_2O_8^{2-} + h\nu \rightarrow 2SO_4^{\cdot-} \tag{1}$$

$$SO_4^{\cdot-} + H_2O \rightarrow SO_4^{2-} + HO^{\cdot} + H^{+} \quad (\text{at all pHs}) \tag{2}$$

$$SO_4^{\cdot-} + OH^{-} \rightarrow SO_4^{2-} + HO^{\cdot} \quad (\text{mostly in alkaline pHs}) \tag{3}$$

$$\text{and } H_2O_2 + h\nu \rightarrow 2HO^{\cdot} \tag{4}$$

To the best of our knowledge, there is no report in the literature related to the application of the photo-persulfate method in removing SA. In a work, dealing with degradation of SA with UV/H_2O_2 process, a 250 W light irradiation source has been used and 92% degradation efficiency has been achieved after 700 min [14].

In this work, considering SA as a target pollutant, the performance of the UV/KPS and UV/H_2O_2 processes are investigated using just a 6 W irradiation source in an efficient falling film photo-reactor. The effects of pH and concentration of the oxidants are studied. Based on HPLC analysis, the kinetics of the reactions are investigated, and from total organic carbon (TOC) analysis, the extent of the substrate mineralization is followed. For UV/KPS process, the role of active radicals is studied using radical scavengers of ethanol (EtOH) and tert-butyl alcohol (t-BuOH). Also, the energy consumption for the both processes are evaluated and compared with previous works.

2. Experimental

2.1. Chemicals and reagents

The substrate SA (99% purity) was purchased from Sigma-Aldrich. H_2O_2 (30% w/w), KPS (≥99%), 0.1 N solution of NaOH, prepared from Merck pellets GR for analysis (99–100%), 0.1 N solution of HCl (prepared from Merck stock solution of 37%, extra pure), orto-phosphoric acid (Merck, ≥85%), and acetonitrile (HPLC grade ≥99.9%) were all purchased from Merck and all aqueous solutions were prepared using deionized water with conductivity less than 0.08 μS/cm.

2.2. Reactor setup and procedure

All the experiments were run in a stainless steel reactor, schematically shown in Fig. 1 [15]. The light source was a UV-C (6 W, Philips) which was placed horizontally in a quartz tube at the center of the reactor. The reactor was equipped with a stainless steel water flow coil, containing a flow from an external thermostat bath (Julabo-F12 ED, Germany) which could adjust temperature with an accuracy of ±0.1˚C. All the experiments were performed at a constant temperature of 25˚C, which was close to the ambient temperature (22 ± 2˚C).

To perform each experiment, a solution (1 L) with an initial concentration of 30 mg/L of SA (0.22 mM) was prepared. After addition of appropriate KPS (corresponding to desired persulfate concentration) or H_2O_2, the solution pH was adjusted to a desired value

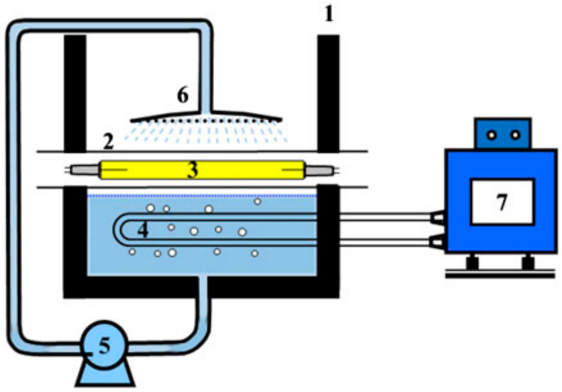

Fig. 1. The used photo-reactor setup; 1: reactor, 2: quartz tube, 3: UV lamp, 4: temperature regulating coil, 5: pump, 6: distributor, and 7: thermostat.

with 0.1 M sodium hydroxide or hydrochloric acid solution with the aid of a pH meter (UB-10, Denver). The solution was transferred into the reactor. To initiate the process, the lamp was turned on and samples (4 mL) were withdrawn at regular times to analyze the processes efficiency at different times.

2.3. Analytical method

Using a UV–vis spectrophotometer (Jasco, V-630), the spectrum of each sample was obtained. The UV–vis spectrum of SA solutions shows a λ_{max} at 298 nm for which the intensity of the relevant peak is declined during the processes (Fig. 2). However, measuring absorbance at this wavelength may not be related to just SA concentration due to the overlap of generated aromatic intermediates. Indeed, absorbance at 298 nm is relevant to all aromatic content in the solution, initiated from SA [14]. Therefore, the measured absorbance at this wavelength can provide a direct and easy way to follow the extent of "aromatics degradation" by the processes. In this regard, the aromatic content degradation efficiency (X) was calculated from:

$$X = \frac{A_0 - A_t}{A_0} \tag{5}$$

where A_0 and A_t are the appropriate aromatic groups absorption at initial time and at any reaction time, t, respectively. Considering this case, optimization of the process was done based on obtained X values, but aiming to find other important criteria, complementary analysis with HPLC (for kinetic study) and TOC (for mineralization assessment) was performed.

The HPLC (SYKAM, Germany) was equipped with a column (Nucleosil C18, 4.6 mm × 250 mm) and UV spectrophotometer as a detector (set at 298 nm), and the mobile phase was a mixture of phosphoric acid and acetonitrile in the ratio of 35:65 conducted with the flow rate of 0.4 mL min^{-1}. Further, the TOC of samples was measured by means of a TOC meter (multi, N/C 3100, Germany).

3. Results and discussion

3.1. Initial pH dependency

pH is an important parameter in degradation and often alters the performance of AOPs. Fig. 3 demonstrates the related obtained aromatics degradation efficiency in UV/KPS and UV/H_2O_2 processes within the initial pH range of 2–10. For UV/KPS, the highest efficiency is obtained at an initial pH of 6, and it decreased mildly with either an increase or a decrease in pH. There are some similar reports in literature, relevant to these observations [13,15,16].

At alkaline pHs,$SO_4^{\bullet -}$ species undergo reactions with OH^- to generate $HO^{\bullet}$ radicals according to Eq. (3). Despite the $SO_4^{\bullet -}$ conversion to SO_4^{2-}, and producing $HO^{\bullet}$ radicals with the redox potential of 2.8 V [17], which is slightly higher than the redox potential of $SO_4^{\bullet -}$, the presence of additional SO_4^{2-} ions can inactivate $HO^{\bullet}$ and $SO_4^{\bullet -}$ species [15,18]. In addition, carbon dioxide formed from the organic content mineralization can lead to the formation of bicarbonate and

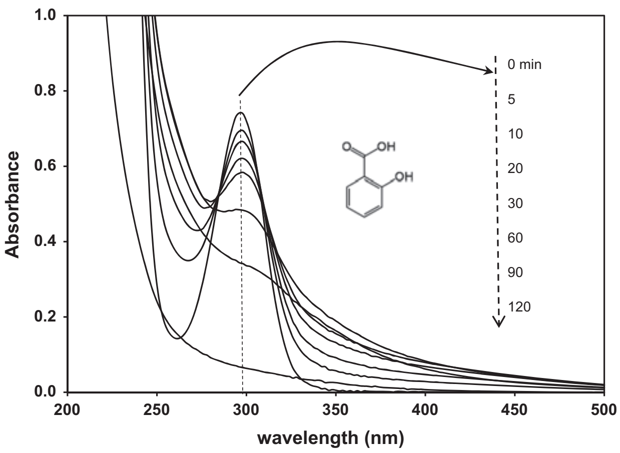

Fig. 2. UV–vis spectrum of SA at different times of UV/KPS process; $[SA]_0 = 30$ mg/L, $[PS] = 1{,}000$ mg/L and pH 6.

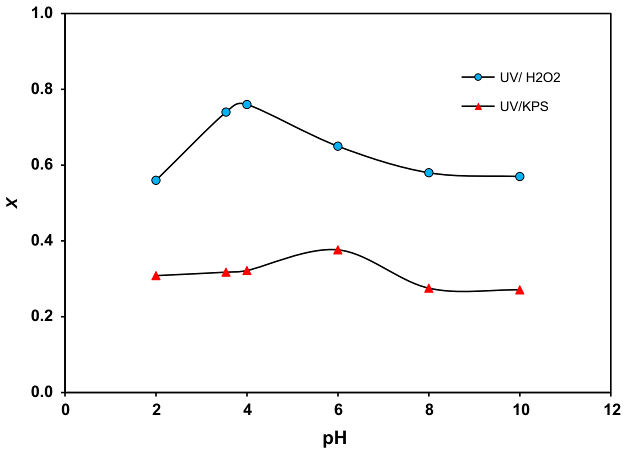

Fig. 3. Effect of initial pH on aromatics removal efficiency of UV/KPS and UV/H_2O_2 processes; $[SA]_0 = 30$ mg/L, $[PS] = 500$ mg/L, $[H_2O_2] = 90$ mg/L and $t = 120$ min.

carbonate ions (as radical scavengers) under alkaline pHs [19]. On the other hand, at acidic pHs, additional $SO_4^{\bullet -}$ is formed with acid catalyzation, according to the following equations [20]:

$$S_2O_8^{2-} + H^+ \rightarrow HS_2O_8^- \tag{6}$$

$$HS_2O_8^- \rightarrow 2SO_4^{\bullet -} + H^+ \tag{7}$$

The extra generated persulfate radicals cause higher radical concentrations, which may favor radical with radical reactions, instead of radicals with present organic pollutants [16].

For UV/H_2O_2 process, efficiency shows a maximum around initial pH of 4 (natural pH of SA solution) and similar to a previous investigation [14], the efficiency decreased with either an increase or a decrease in pH. At alkaline pHs, the redox potential of hydroxyl radicals is decreased. Also, hydrogen peroxide may undergo self-decomposition into water and oxygen at high pH levels, as follows [21]:

$$2H_2O_2 \rightarrow 2H_2O + O_2 \tag{8}$$

Also, under regressive acidic media, H_2O_2 molecules will react with excessive H^+ ions to form oxonium ions ($H_3O_2^+$), which are stable and under UV irradiation cannot form $HO^{\bullet}$radicals [22]. At the same time, the generated hydroxyl radicals may be scavenged by the excess H^+ ions [23]. From Fig. 3, it is also obvious that UV/H_2O_2 process exhibits a higher variation with pH, within the used range.

It is noteworthy that according to Eqs. ((2) and (3)), $H^+$is released while HO^- ion is consumed in UV/KPS process; so, the solution pH is expected to decrease as reaction proceeds with time [15] (Fig. 4); however, in UV/H_2O_2 process, the value of pH remains almost constant (only a decrease of 0.3 was appropriate after 120 min treatment), due to no stable ion generation/consumption, in contrary to the UV/KPS process.

From the above results, optimal initial pH for the operation of UV/KPS and UV/H_2O_2 processes were considered as 6 and 4, respectively.

3.2. Effect of oxidants initial concentration

Effect of persulfate and hydrogen peroxide concentrations was investigated at the relevant optimum pH. The results depicted in Fig. 5 are corresponding to 120 min treatments. As it is observed, increase in PS concentration up to about 1,000 mg/L causes considerable efficiency improvement, due to more reactive radical generation, according to Eqs. ((1)–(3)). It is observed that higher PS concentrations does not result in significant change in the efficiency, perhaps due to the retarding effect of excessive generated reactive radicals recombination or reaction with persulfate ions which act as a scavenger at excess concentrations [12,16]. Hence, the optimal value for PS is about 1,000 mg/L (5.2 mM) at which a high efficiency of 94% can be achieved after 120 min and the persulfate retarding effect is prevented.

A similar trend of variations is observed for hydrogen peroxide dosage, but at much lower concentration levels (Fig. 5). Obviously, UV/H_2O_2 process is much more sensitive to the oxidant dosage, compared with the UV/KPS process.

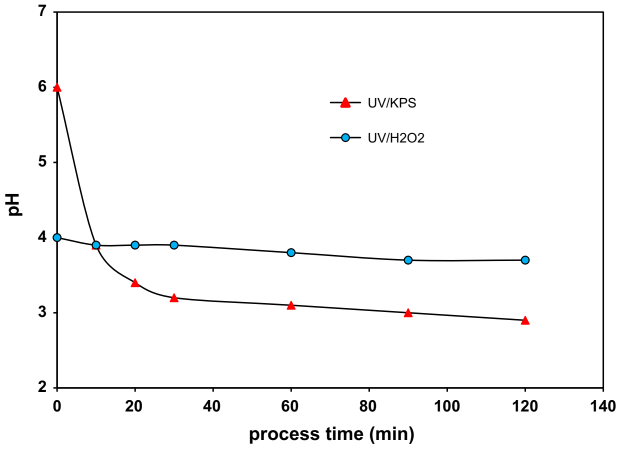

Fig. 4. Variation of solution pH during reaction for both the processes; $[SA]_0 = 30$ mg/L, $[PS] = 500$ mg/L, $[H_2O_2] =$ 90 mg/L.

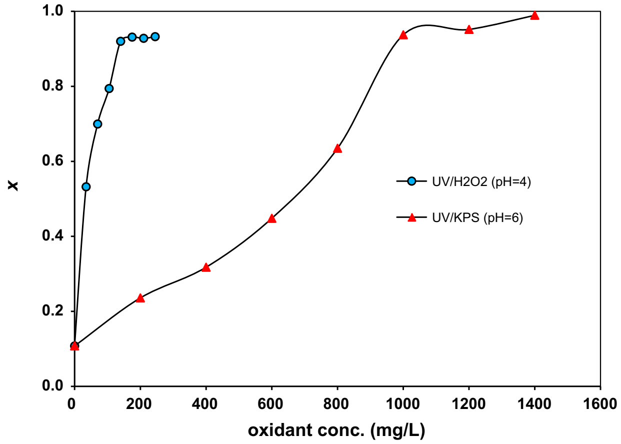

Fig. 5. Influence of the oxidants concentration on the removal efficiency; $[SA]_0 = 30$ mg/L, $t = 120$ min.

It can be seen that beyond 140 mg/L (4.2 mM) of hydrogen peroxide, no more efficiency is achieved in UV/H_2O_2 process. The reason can be the self-quenching of $HO^{\bullet}$ radicals by extra amounts of H_2O_2 molecules that generate less reactive $HO_2^{\bullet}$ radicals [24]:

$$H_2O_2 + HO^{\bullet} \rightarrow H_2O + HO_2^{\bullet} \tag{9}$$

Using 140 mg/L of hydrogen peroxide, 93% efficiency was achieved after 120 min under the initial natural pH of 30 mg/L of SA (pH 4). It is noteworthy that, as intercept in Fig. 5 shows, in the absence of any oxidant, UV light irradiation alone causes only about 10% efficiency of the aromatics group degradation.

3.3. The role of radical species

To assess the contribution of sulfate and hydroxyl radicals in the efficiency of UV/KPS process, two alcoholic radical scavengers, EtOH and t-BuOH, were added into the solutions separately. EtOH can quench both hydroxyl and sulfate radicals; whereas, t-BuOH can mainly scavenge hydroxyl radicals and poorly react with sulfate radicals [25,26]. Accordingly, difference in efficiencies in the presence of these scavengers can be considered as sulfate radicals' contribution.

As Fig. 6 shows, addition of EtOH at different amounts has diminished the efficiency much more than t-BuOH. Addition of 1.4% (V/V) of EtOH or t-BuOH, for instance, has reduced the efficiencies to 66% and 37%, respectively; compared with the normal operations without scavengers. These observations imply that both radical species are effective in the degradation process, and the average contribution of hydroxyl and sulfate radicals is about 56% and 44%, respectively. It is notable that $SO_4^{\bullet -}$ species has been known to be more selective for electron transfer reactions, while $HO^{\bullet}$ radicals can rapidly take part in hydrogen addition or abstraction reactions [16].

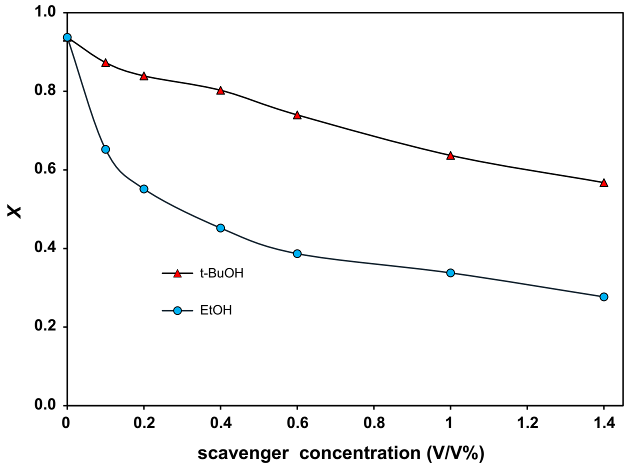

Fig. 6. Influence of scavengers on degradation efficiency; $[SA]_0 = 30$ mg/L, [PS] = 1,000 mg/Land $t = 120$ min.

3.4. Kinetic study

As mentioned in analytical method section, decline of absorbance intensity at $\lambda_{\max}$ of 298 nm is attributed to the total aromatics degradation. So, for SA degradation kinetic study, the HPLC analysis was used to follow the concentration of SA in the employed processes. The peaks related to the SA molecules appeared at the retention time of 8.40 min (Fig. 7(a)–(f)), and as expected, the corresponding intensity decreases with reaction time. The concentration of SA for each chromatogram was obtained using a calibration standard curve, based on the area under the peaks.

The variation of SA concentration vs. time is presented in Fig. 8. After 60 min degradation, efficiency reaches to 94 and 98% in UV/KPS and UV/H_2O_2 processes, respectively. Also, the inset figure shows that the trends of SA degradation vs. time can be fitted adequately well with a pseudo-first-order kinetic model as:

$$\ln \frac{[SA]_0}{[SA]_t} = kt \tag{10}$$

where $[SA]_0$, $[SA]_t$, and k refer to the initial concentration of SA, SA concentration at any time, and the kinetic rate constant, respectively. From the slope of the curves, the rate constants were obtained as 0.049 and 0.066 min^{-1} for UV/KPS and UV/H_2O_2 processes, respectively. Here, the degradation efficiency is defined as: $X = \{[SA]_0 - [SA]_t\}/[SA]_0$

3.5. Mineralization assessment

TOC analysis can provide a criterion to follow the extent of mineralization. In this regard, under the obtained optimal conditions of the processes, TOC values were measured at different times. The TOC results are presented in Fig. 9((a) and (b)) for comparison with SA and aromatic degradation efficiencies. The efficiency based on TOC was defined for this case as: $X = (TOC_0 - TOC_t)/TOC_0$, where TOC_0 and TOC_t represent the corresponding values at initial and at a time t.

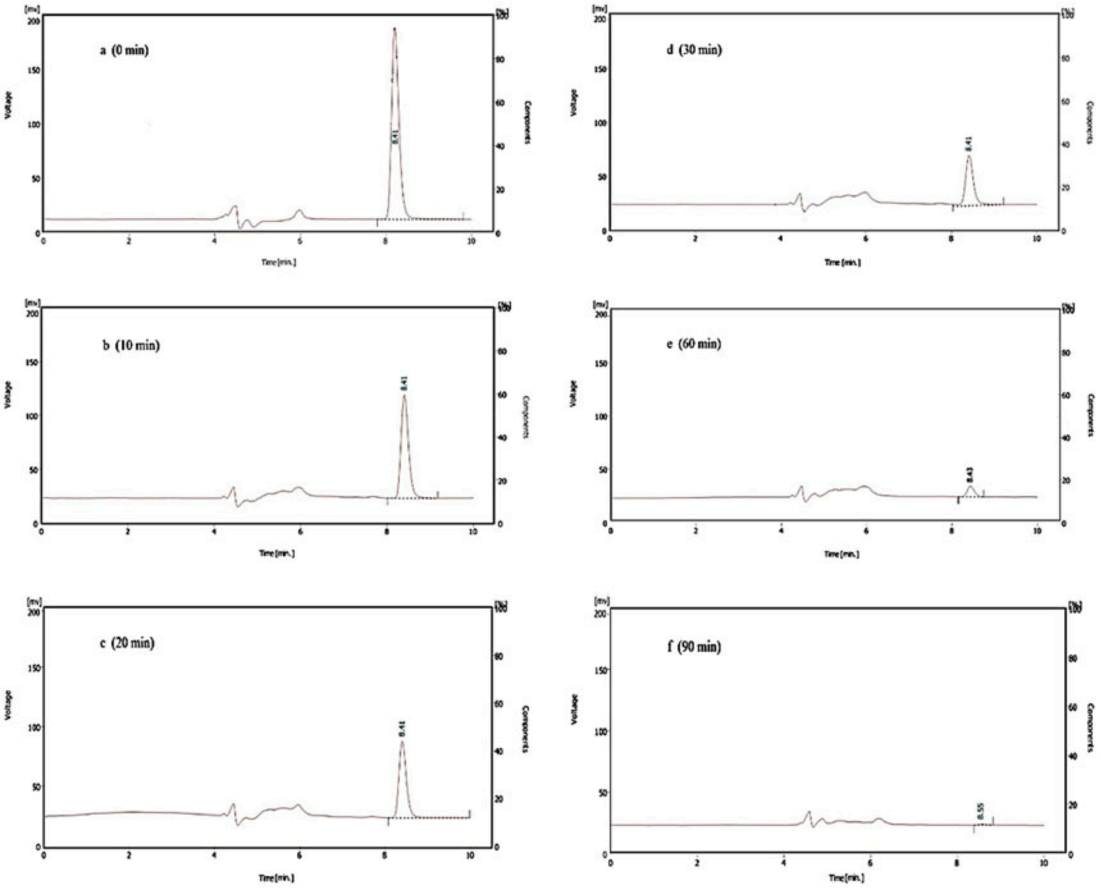

Fig. 7. HPLC chromatogram spectra at different process times during UV/KPS process (a: 0 min, b: 10 min, c: 20 min, d: 30 min, e: 60 min, and f: 90 min) for SA detection; $[SA]_0$ = 30 mg/L, [PS] = 1,000 mg/L and pH 6.

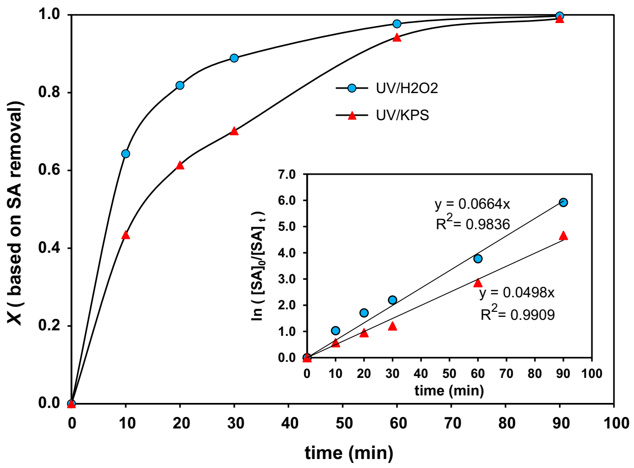

Fig. 8. Variation of SA degradation with time; $[SA]_0 = 30$ mg/L, ([PS] = 1,000 mg/L at pH 6), and ($[H_2O_2] = 140$ mg/L at pH 4).

A remarkable difference is observed for the progress of just SA, aromatics and TOC efficiencies for both the processes. As Fig. 9(a) shows for UV/KPS process, when the removal of SA is nearly completed, the aromatics and TOC removals have much delay, and no mineralization is relevant before about 30 min. It implies that PS action is rather selective, where it first reacts with SA molecules and then with aromatic species, and after that with all present organics toward their mineralization after first 10 minutes. The lack of delay in UV/H_2O_2 process (Fig. 9(b)), on the other hand, can be attributed to the nonselective oxidation behavior of hydroxyl radicals [16].

After a longer time of 120 min treatment, about 80 and 87% mineralization is achieved in UV/KPS and UV/H_2O_2 processes, respectively. Also, based on presented data, and the trend of variations, despite the higher SA degradation rate in the UV/H_2O_2 process, nearly perfect aromatic degradation as well as mineralization is achieved, in shorter times, with UV/KPS process.

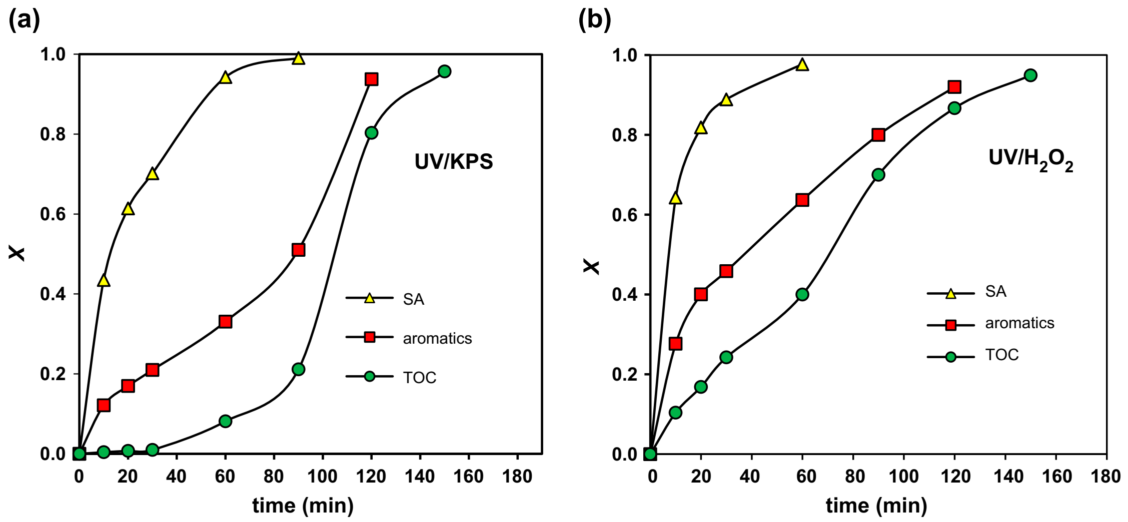

Fig. 9. Different criteria in UV/KPS (a) and UV/H_2O_2 (b) processes; $[SA]_0 = 30$ mg/L, ([PS] = 1,000 mg/L at pH 6) and ($[H_2O_2] = 140$ mg/L at pH 4).

Irrespective of the kind of used oxidants, concerning the function of hydroxyl radical, which is generated in a large extent in the both processes, a number of intermediates have been introduced in previous investigations which ultimately lead to perfect mineralization [4,27]. The SA undergoes parallel degradations in the presence of hydroxyl radical. A part of it changes into phenol through decarboxylation, while the others turned into 2,3-dihydroxybenzoic acid or 2,4-dihydroxybenzoic acid. Phenol is then further oxidized to catechol which will be further converted into intermediates and into p-benzoquinone. Then, maleic acid and fumaric acid are appeared following the benzene ring opening in both the parallel branches. In addition, these two species will transform into smaller molecule acids such as succinic acid, malonic acid, oxalic acid, acetic acid, and formic acid. The last step is the mineralization of the different small molecule compounds, which ultimately convert to CO_2 and H_2O.

3.6. Energy consumption

Among several factors for the superiority of a wastewater treatment technology, economic is often vital [28]. In this regard, electrical energy consumption (E_{EC}) is the main part of energy in photochemical process. Here, E_{EC} can be calculated according to the photochemistry commission proposal of the International Union of Pure and Applied Chemistry for the first-order degradations, as [29]:

$$E_{EC} = \frac{1{,}000 \times P \times t}{60\ V \log\{[SA]_0/[SA]_t\}} \tag{11}$$

where P is the electric power (kW) of the photochemical system (generally aimed the irradiation energy), V is the volume (L) of the solution in the reactor, and t is the reaction duration time (min). To take into account the impact of reaction temperature variation on the E_{EC} calculations, Eq. (11) can be modified, noting that $\ln\{[SA]_0/[SA]_t\}/t$ represents the rate constant k (unit of min^{-1}); therefore,

$$E_{EC} = \frac{38.4 \times P}{V \times k} \tag{12}$$

Thus, the required E_{EC} for the photochemical degradation of SA solution with UV/KPS and UV/H_2O_2 processes are 77.1 and 57.8 kWh/m^3, respectively. Considering the electrical energy price in US market, 0.068 US$/kWh (in 2013) [30], the electrical energy cost for both processes will be about 5.2 and 3.93 US $/$m^3$, respectively.

For the aim of process evaluation, the applied two processes were compared with a relevant work, reported by Zanta and Martínez-Huitle [14] on the degradation of SA, including UV/Fenton and UV/H_2O_2 processes. With respect to the close SA final degradation efficiency (within 92–98%) in this work and theirs, the irradiation electrical energy consumption per unit volume and per unit initial SA concentration,

Table 1
The performance comparison of different processes for SA degradation

Process	$[SA]_0$ (mg/L)	Oxidant (mg/L)	Lamp (W)	Time (min)	X (%)	E_{EC} (kWh/m^3)	SEC (kWh/mg)	Ref.
UV/Fenton	1,000	1,468	250	150	98	2.4×10^4	2.5×10^{-3}	[14]
UV/H_2O_2	1,000	1,468	250	700	92	1.7×10^5	1.2×10^{-2}	[14]
UV/KPS	30	1,000	6	60	94	77.11	2.0×10^{-4}	This work
UV/H_2O_2	30	140	6	60	98	57.83	2.0×10^{-4}	This work

the specific energy consumption (SEC), can be evaluated via equation:

$$\text{SEC} = \frac{p \times t}{V \times [\text{SA}]_0} \tag{13}$$

SEC, in fact, signifies the amount of electrical energy consumption (kWh) per unit mass of treated substrate (mg of SA). Table 1 shows that SEC values in this work are one or two orders of magnitude less than those in the other work (relevant conditions are given). Even adding the circulating pump energy consumption does retain the significant preference of the used process. The high performance of the used photo-reactor, due to proper UV utilization for activating the processes, provides this significant advantage.

4. Conclusions

In this study, two photochemical oxidation processes were examined for the degradation of 30 mg/L of SA in aqueous media. Concisely, the following items are concluded: (i) under optimum conditions by UV/KPS and UV/H_2O_2 processes, 94 and 93% of total aromatics can be degraded after 120 min; (ii) the UV/KPS and UV/H_2O_2 processes have their highest efficiencies under the initial pH and oxidants concentration of 6 and 1,000 mg/L, and 4 and 140 mg/L, respectively; (iii) degradation of SA, with 94 and 98% efficiencies, respectively, is obtained after 60 min; however, for 80 and 87% mineralization, much longer time, about 120 min, is required; (iv) for UV/KPS process, application of radical scavengers showed that both sulfate and hydroxyl radicals are active in degradation; (v) the rate of SA degradation matches adequately well with pseudo-first-order kinetic model; (vi) despite a higher SA degradation rate in the UV/H_2O_2 process, for perfect aromatic degradation, as well as mineralization, the UV/KPS process is preferred (irrespective of the amount of oxidants); (vii) for nearly complete degradation of SA molecules by the UV/KPS and UV/H_2O_2 processes, 77.1 and 57.8 kWh/m^3 electrical energy are required, respectively; and (viii) the used processes were evaluated in comparison with a previous work and much preference was shown in terms of energy and oxidant consumption, as well as treatment duration time.

Acknowledgment

The authors wish to acknowledge the Bu-Ali Sina University authorities for providing the financial support to carry out this work.

References

[1] Y. Gao, N. Gao, Y. Deng, Y. Yang, Y. Ma, Ultraviolet (UV) light-activated persulfate oxidation of sulfamethazine in water, Chem. Eng. J. 195–196 (2012) 248–253.

[2] M. Klavarioti, D. Mantzavinos, D. Kassinos, Removal of residual pharmaceuticals from aqueous systems by advanced oxidation processes, Environ. Int. 35 (2009) 402–417.

[3] V. Naddeo, L. Rizzo, V. Belgiorno, Water, wastewater and soil treatment by advanced oxidation processes, Aster Publisher, Fisciano, SA, 2010.

[4] E. Guinea, C. Arias, P.L. Cabot, J.A. Garrido, R.M. Rodríguez, F. Centellas, E. Brillas, Mineralization of salicylic acid in acidic aqueous medium by electrochemical advanced oxidation processes using platinum and boron-doped diamond as anode and cathodically generated hydrogen peroxide, Water Res. 42 (2008) 499–511.

[5] K. Kümmerer, Pharmaceuticals in the Environment, Springer, Berlin, 2001.

[6] S. Su, W. Guo, C. Yi, Y. Leng, Z. Ma, Degradation of amoxicillin in aqueous solution using sulphate radicals under ultrasound irradiation, Ultrason. Sonochem. 19 (2012) 469–474.

[7] J. Chung, J.O. Kim, Application of advanced oxidation processes to remove refractory compounds from dye wastewater, Desalin. Water Treat. 25 (2011) 233–240.

[8] S.Y. Yang, Y.Y. Chen, H.Z. Xu, P. Wang, Y.H. Liu, M.D. Wang, A novel advanced oxidation technology: Activated persulfate, Prog. Chem. 20 (2008) 1433–1438.

[9] M.H. Habibi, B. Karimi, Nanostructure Cu–Zn mixed-oxide supported photocatalyst fabricated by impregnation method for the photocatalytic degradation of C.I. Reactive Orange 16 (V3R)in water, Spectrochim. Acta, Part A 124 (2014) 629–631.

[10] V. Maurino, P. Calza, C. Minero, E. Pelizzetti, M. Vincenti, Light-assisted 1,4-dioxane degradation, Chemosphere 35 (1997) 2675–2688.

[11] ERA. Weiner, Dictionary of inorganic water quality parameters and pollutants, in: Applications of Environmental Chemistry, Lewis Publishers, CRC Press LLC, Boca Raton, FL, 2000, (Chapter 7), p. 231.

[12] T.K. Lau, W. Chu, N.J.D. Graham, The aqueous degradation of butylated hydroxyl anisole by $UV/S_2O_8^{2-}$: Study of reaction mechanisms via dimerization and mineralization, Environ. Sci. Technol. 41 (2007) 613–619.

[13] D. Salari, A. Niaei, S. Aber, M.H. Rasoulifard, The photooxidative destruction of CI Basic Yellow 2 using $UV/S_2O_8^{2-}$ process in a rectangular continuous photoreactor, J. Hazard. Mater. 166 (2009) 61–66.

[14] C.L.P.S. Zanta, C.A. Martínez-Huitle, Degradation of 2-hydroxybenzoic acid by advanced oxidation processes, Braz. J. Chem. Eng. 26 (2009) 503–513.

[15] J. Saien, A.R. Soleymani, J.H. Sun, Parametric optimization of individual and hybridized AOPs of Fe^{2+}/H_2O_2 and $UV/S_2O_8^{2-}$ for rapid dye destruction in aqueous media, Desalination 279 (2011) 298–305.

[16] G.R. Peyton, The free-radical chemistry of persulfate-based total organic carbon analyzers, Mar. Chem. 41 (1993) 91–103.

[17] G.V. Buxton, C.L. Greenstock, W.P. Helman, A.B. Ross, Critical review of rate constants for reactions of hydrated electrons, hydrogen atoms and hydroxyl radicals ($HO^{\bullet}/O^{\bullet}$) in aqueous solution, J. Phys. Chem. Ref. Data 17 (1988) 513–531.

[18] E. Lipczynska-Kochany, G. Sprah, S. Harms, Influence of some groundwater and surface waters constituents on the degradation of 4-chlorophenol by the Fenton reaction, Chemosphere 30 (1995) 9–20.

[19] S.C. Xu, H.D. Zhou, X.Y. Wei, J. Lu, The pH dependence and effects of the oxidative products of some aromatic compounds in ozonation under UV irradiation, Ozone Sci. Eng. 11 (1989) 281–296.

[20] D.A. House, Kinetics and mechanism of oxidations by peroxydisulfate, Chem. Rev. 62 (1962) 185–203.

[21] C. Zhou, N. Gao, Y. Deng, W. Chu, W. Rong, S. Zhou, Factors affecting ultraviolet irradiation/hydrogen peroxide (UV/H_2O_2) degradation of mixed N-nitrosamines in water, J. Hazard. Mater. 231–232 (2012) 43–48.

[22] N.K. Daud, B.H. Hameed, Decolorization of Acid Red 1 by Fenton-like process using rice husk ash-based catalyst, J. Hazard. Mater. 176 (2010) 938–944.

[23] X.R. Xu, Z.Y. Zhao, X.Y. Li, J.D. Gu, Chemical oxidative degradation of methyl tert-butyl ether in aqueous solution by Fenton's reagent, Chemosphere 55 (2004) 73–79.

[24] C.H. Liao, S.F. Kang, F.A. Wu, Hydroxyl radical scavenging role of chloride and bicarbonate ions in the H2O2/UV process, Chemosphere 44 (2001) 1193–1200.

[25] G.P. Anipsitakis, D.D. Dionysiou, Radical generation by the interaction of transition metals with common oxidants, Environ. Sci. Technol. 38 (2004) 3705–3712.

[26] A. Ghauch, A.M. Tuqan, Oxidation of bisoprolol in heated persulfate/H_2O systems: Kinetics and products, Chem. Eng. J. 183 (2012) 162–171.

[27] Q. Dai, Y. Xia, L. Jiang, W. Li, J. Wang, J. Chen, Enhanced degradation of aspirin by electrochemical oxidation with modified PbO_2 electrode and hydrogen peroxide, Int. J. Electrochem. Sci. 7 (2012) 12895–12906.

[28] A.R. Khataee, M. Safarpour, M. Zarei, S. Aber, Combined heterogeneous and homogeneous photodegradation of a dye using immobilized TiO_2 nanophotocatalyst and modified graphite electrode with carbon nanotubes, J. Mol. Catal. A: Chem. 363–364 (2012) 58–68.

[29] J.R. Bolton, K.G. Bircher, W. Tumas, C.A. Tolman, Figures-of-merit for the technical development and application of advanced oxidation technologies for both electric- and solar-driven systems, Pure Appl. Chem. 73 (2001) 627–637.

[30] http://www.eia.gov (US Government Energy Information Administration, Independent Statistics and Analysis).